2024 IEEE International Conference on Robotics and Automation (ICRA 2024)
May 13-17, 2024. Yokohama, Japan

Acoustically Driven Micropipette for Hydrodynamic Manipulation of Mouse Oocytes

Zhaofeng Zuo, Xiaoming Liu, *Member, IEEE,* Zhuo Chen, Yuyang Li, Xiaoqing Tang, Dan Liu, Qiang Huang, *Fellow, IEEE,* and Tatsuo Arai, *Life Fellow, IEEE*

Abstract— **Micromanipulation techniques that can achieve controlled fine operations at the micro scale play an important role in biomedical fields including embryo engineering, gene engineering, drug screening, and cell analysis. However, micromanipulation of biological micro-objects, such as cells and micro tissues, suffers from mechanical damage and low efficiency. Several techniques have been introduced to manipulate cells more easily, but most of them are restricted by expensive devices, limited work area, and potential damage to cellular structure. Here we develop a hydrodynamic manipulation method to rotate and transport mouse oocytes, which utilizes acoustic waves and micropipette to generate acoustic radiation force and excite microstreaming. This method can accomplish rotational and translational operations precisely and controllably. We tested the process of trapping, rotation, and transportation of the mouse oocytes, and measured rotational and translational speed with a range of applied voltage. The method was able to shorten the cost time of delivery and posture adjustment before oocyte injection. Our study provides an easy-to-use technique for oocyte manipulation without contact, and it has the potential to be universally applied in many cellular studies.**

I. Introduction

Micromanipulations of cells have gained popularity in clinical and biology fields, such as embryo engineering [1], gene engineering [2], [3], drug screening [4], and cell analysis [5], [6]. Controlled transportation and rotation are essential operations that micromanipulation methods execute for cells and microtissues [7]. For instance, in the intracellular injection operation of the oocyte, a pair of micropipettes is needed by the operators [8]. One is used to fix and transport the oocyte, and another can manually rotate the oocyte at an appropriate posture before injection, which preserves the polar body from the invasive site and increases the survival and fertilization rate [9]. However, cellular structures are fragile, and the damage caused by mechanical contact is inevitable in the operation process. Additionally, it is difficult for manipulators to allow the out-of-plane rotation because of the limited depth of field under a microscope, which needs time to aspirate and release the oocyte repeatedly. Therefore, the traditional manual operation has several restrictions, such as low efficiency and potential damage caused by the invasive manipulation. Hence, techniques are required to manipulate the oocyte efficiently and safely.

In recent years, several techniques that can manipulate micro-objects have been introduced to fulfill translational or rotational operations. Robotic manipulation methods using computer visual servo were introduced to manipulate micro targets, which used the injection pipette to automatically deform the cell and apply small rotation force by modeling and path planning [10], [11]. However, this invasive method needs precise motorized micromanipulators, which is expensive and not friendly for untrained operators. Also, mechanical contact is prone to harm delicate biological targets. Magnetic tweezers were reported to manipulate cells by utilizing the magnetic field, which actuated magnetic microrobots to exert force on the targets [12], [13]. Although magnetic fields are flexible and safe for cellular structures because of nonmechanical contact, the techniques have a limited work area and need to develop and adjust complicated devices such as magnetic coils, which highly restrict their applications. Optical tweezers generate highly focused laser beams, and cells will be rotated remotely and precisely by the optical trapping force while exposed to the changed beam point [14]. However, the range of optical tweezers is limited to the focal point of the laser beam, which means that the trapped objects must be operated within a certain plane [15]. In addition, if the laser intensity cannot reach a relatively high level, the force is not enough to manipulate cells, but the too-high power may result in increasing temperature and influence cell activity [16]. Recently, fluidic operation through acoustic waves has been expected as a promising micromanipulation method with biocompatibility, multiple rotational functions, and flexible operation [17]–[21]. Nevertheless, the fabrication of microfluidic devices is a time-consuming process, and the new operators need time to be familiar with it quickly [22]. Thus, it is essential to develop an acoustic-fluidic hybrid technique with good usability in an open environment, which can not only transport the cells with strong positional stability and a large movement range but also achieve high accuracy and velocity-controlled operations of rotation.

This work was supported by the National Natural Science Foundation of China under Grant 62273052, the Beijing Natural Science Foundation under Grant IS23062, China Postdoctoral Science Foundation under Grant 2022M710378 and the Grant-in-Aid for Scientific Research under Grant 22H01441 from the Ministry of Education, Culture, Sports, Science and Technology of Japan. (Corresponding author: Xiaoming Liu.)

Z. Zuo, X. Liu, X. Tang, D Liu, Y Li, Z Chen, Q. Huang and T. Arai are with the Key Laboratory of Biomimetic Robots and Systems, Ministry of Education, State Key Laboratory of Intelligent Control and Decision of Complex System, Beijing Advanced Innovation Center for Intelligent Robots and Systems, and School of Mechatronical Engineering, Beijing Institute of Technology, Beijing 100081, China (e-mail: liuxiaoming555@ bit.edu.cn).

T. Arai is also with Center for Neuroscience and Biomedical Engineering, The University of Electro-Communications, Tokyo 1828585, Japan.

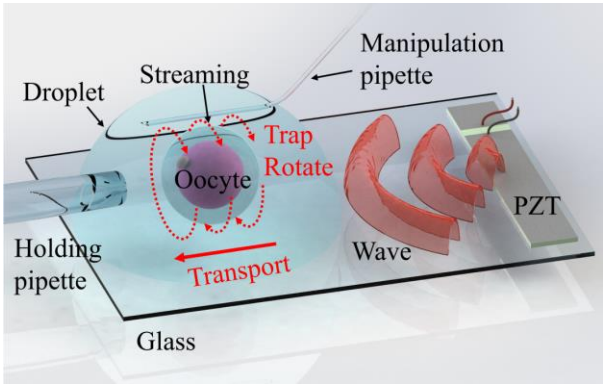

Figure 1. Schematic of hydrodynamic manipulation of mouse oocytes by acoustic waves.

Here, we present a hydrodynamic manipulation method utilizing the acoustically driven micropipette to generate microstreaming in its vicinity under the acoustic field, which can achieve precise trapping and transporting operations of biological targets without invasion. Several previous researches have generated regular streaming and achieved cellular manipulation by fixing the acoustic source to the pipettes[7], [23]. The difference we have is that the acoustic source is attached to the object space, which makes the micropipette removable and the whole system reusable. As shown in Fig. 1, the piezoelectric transducer (PZT) can emit acoustic waves by vibration. Due to the existence of solid-liquid interface, the vicinity of micropipette can generate hydroacoustic flow and acoustic radiation force when exposed to acoustic waves, which can trap and rotate oocytes in a medium droplet. The micropipette was mounted on micromanipulators to allow high-resolution transportation over a 10×10 mm area. In the experiments, we verified the most appropriate excitation frequency by sweeping, then measured the rotational velocities of the oocyte in different driven voltages of the piezoelectric, which can help the operators to precisely control the posture of a single oocyte. In addition, we tested the maximum velocity of oocyte movement in the X and Y axes. Finally, the time consumption of this manipulation approach was compared to the typical method with holding pipettes. The experimental result suggests that this proposed method is efficient, low-cost, biologically friendly, and compatible with existing equipment, which can also have wide applications in single cell operations and analysis.

II. System Design

A. System Setup

Fig. 2 shows the configuration of the acoustic-driven system for manipulating mouse oocytes in an open liquid environment. The manipulation device was established on an inverted microscope (Nikon, Ti2, Japan), which was equipped with an sCMOS camera (PCO, edge 4.2 LT, Germany) to capture images at 30 frames/s. The injection holders (Narishige, HI-9, Japan) were connected to a pair of three degrees of freedom (3-DOF) micromanipulators (Narishige, MMO-4, Japan), which can be controlled by the joystick to achieve precise position and movement of micropipettes. The holding pipette and manipulation pipette were respectively connected with two pneumatic injectors (Narishige, IM-12, Japan). A function generator (GW Instek, AFG-2225, China)

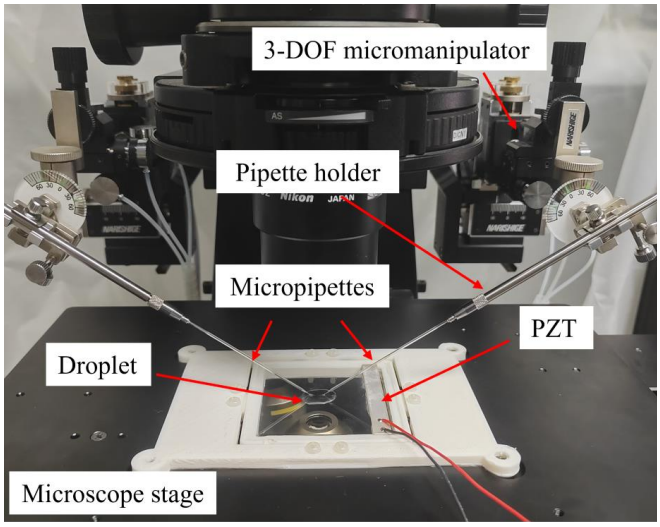

Figure 2. System setup. The image shows compnents of the acoustic-driven system and the device of hydrodynamic manipulation.

was used to send signals at a specific frequency to an amplifier (Aigtek, ATA-2042, China). The output of the amplifier was connected to a PZT (Shenlei, PZT5H-55-7-0.5, China) through wires to apply enough voltage. Glue was used to make the PZT adhere to a glass slide on a 3D printing support, and the whole device was placed on the stage of the microscope.

The Micropipettes were fabricated by pulling borosilicate glass capillaries (Gairdner, B10014N, China) with an outer diameter of 1 mm and an inner diameter of 0.6 mm in the puller (Sutter Instrument, P-1000, America). Then the pipette (the inner diameter of the tip is about 1 μm) was ground by the microgrinder (Narishige, EG-402, Japan) to generate a beveled tip with an inner diameter of about 10-20 μm.

B. Working Mechanism

Unlike the uniform material distribution regions, the interface with a difference in the physical states phase results in apparent specificity in the localized area. For instance, when exposed to an acoustic wave, a gas-liquid interface or a solid-liquid interface will generate regular streaming patterns because of oscillating. In a Newtonian fluid like the culture medium, a pipette oscillates under the surrounding acoustic pressure with a wavelength much larger than its diameter (5-15 μm). The motion of the fluid can be investigated using the standard Navier-Stokes equations for a linear viscous compressible fluid. By assuming the form of the velocity, density, and pressure of the fluid, the N-S equation can be approximated to a first-order governing equation [24]:

$$\frac{\partial \rho_1}{\partial t} + \rho_0(\nabla \cdot \boldsymbol{v_1}) = 0, \tag{1}$$

$$\rho_0 \frac{\partial \boldsymbol{v_1}}{\partial t} = -\nabla p_1 + (\tfrac{4}{3}\mu + \mu_0)\nabla^2 \boldsymbol{v_1} \tag{2}$$

Where ρ, $\boldsymbol{v}$, and p represent the mass density, velocity, and pressure of the fluid, respectively, and the subscripts indicate the corresponding order. μ is the dynamic viscosity, and μ_0 is the bulk viscosity. In addition to the fluidic streaming, the secondary radiation force will appear near the pipette due to scattering the previously absorbed acoustic waves [25], which will change the pressure in the vicinity. The force is capable of

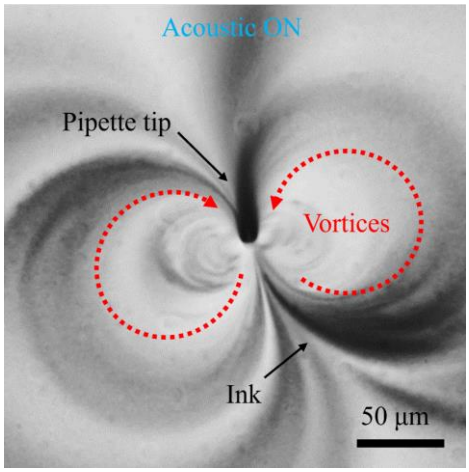

Figure 3. Characterization of the fluidic streaming generated in the acoustic field. The input frequnency is 3.6 kHz. The image plane is perpendicular to the pipette axis.

converging micro-objects to a certain position and trapping them stably. For a microsphere with a radius of R, the equation of secondary radiation force can be expressed as:

$$F_{rad} = -\frac{4\pi R^3}{3}\left(\frac{1}{2}f_1\kappa_0\nabla p_1^2 - \frac{3}{4}\rho_0 f_2\nabla \boldsymbol{v_1^2}\right), \quad (5)$$

$$f_1 = 1 - \frac{\kappa_p}{\kappa_0}, f_2 = 1 - \frac{3\rho_0}{\rho_p+\rho_0}. \quad (6)$$

Where κ and ρ are the compressibility and density of the material, respectively. The subscripts '0' and 'p' indicate the microbeads and their surrounding fluid.

Using carbon ink to visualize the fluidic streaming, it can be observed that the micropipette was driven by the acoustic waves and excited liquid in the vicinity, as shown in Fig. 3. The acoustic streaming patterns are determined by the applied excitation frequency, while the input voltage can only influence the streaming velocity. After the frequency sweeping, we find that the streaming can be generated stably near the tip at about 3.2-3.8 kHz. In particular, with the frequency of 3.6 kHz, two vortices were created symmetrically and the rotation axis was parallel to the micropipette. The vortices can supply torque to rotate the mouse oocyte without any mechanical contact, and this streaming can also capture the oocyte with a certain speed of movement in the horizontal plane or vertical direction.

III. Oocyte Hydrodynamic Manipulation

In the clinical and biology fields, precise posture control and efficient transportation are the fundamental operations of the cells, which is also the essential prerequisite for subsequent execution of cellular surgery, such as intracellular injection. Using the acoustic waves to generate the secondary radiation force near the typical injection pipette, the mouse oocytes were rotated by the near-field force and trapped by the microstreaming. By adhering a PZT to the glass slide, an oocyte operation platform is modified for acoustically manipulating, and all the other equipment can be the same as the traditional equipment, which does not require more training for the operators.

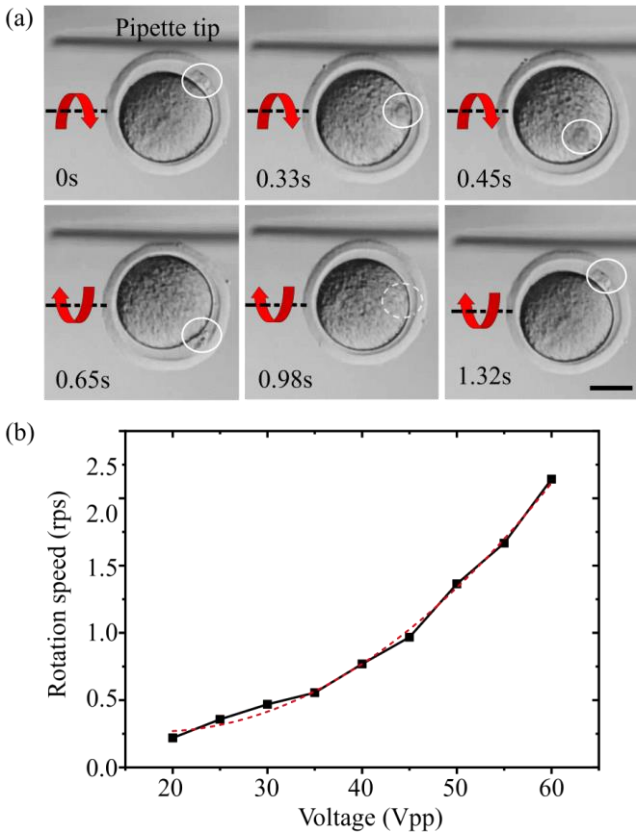

Figure 4. (a) Rotating the oocyte to adjust the posture of angle. Scale bar: 30 μm. (b) Plot of rotation speed against input voltage Vpp with a constant frequency of 3.6 kHz.

A. Trapping and Rotation

The stable rotation is the key to trapping the oocytes and adjusting the posture. The fluidic vortices oscillated by the micropipette provide the torque to drive the cell to rotate in the same direction as the vortices. Manipulating operation is very simple: when activating the acoustic waves, the vicinal target will be attracted to the vortex center and rotated. This motion can be interrupted immediately by turning off the input signal.

There are two vital elements of the input sinusoidal voltage applied on the PZT actuator, the frequency determines the capture position along the micropipette, and the input voltage determines the angular velocity of target rotation. By sweeping the signal, we found that at 3.6 kHz the oocyte could be trapped at the position near the tip but without any contact, which is also the proper position for single-cell operations as shown in Fig. 4(a). This figure also illustrates the image of the single oocyte out-of-plane rotation process. Setting the poly body (white circle) as the feature point of the oocyte, it can be obtained that the change in the angle of oocyte rotation over time is quite stable and fast. Significantly, the positions of the micropipette and the oocyte center were not aligned in the horizontal or vertical planes, but the oocyte was trapping sidelong below the pipette. The reason for this phenomenon can be explained by the position of vortices in Fig. 4, where the streaming centers were also at an inclined plane of the vertical or horizontal directions. The oocyte tends to approach one of the two vortex centers due to acoustic radiation forces,

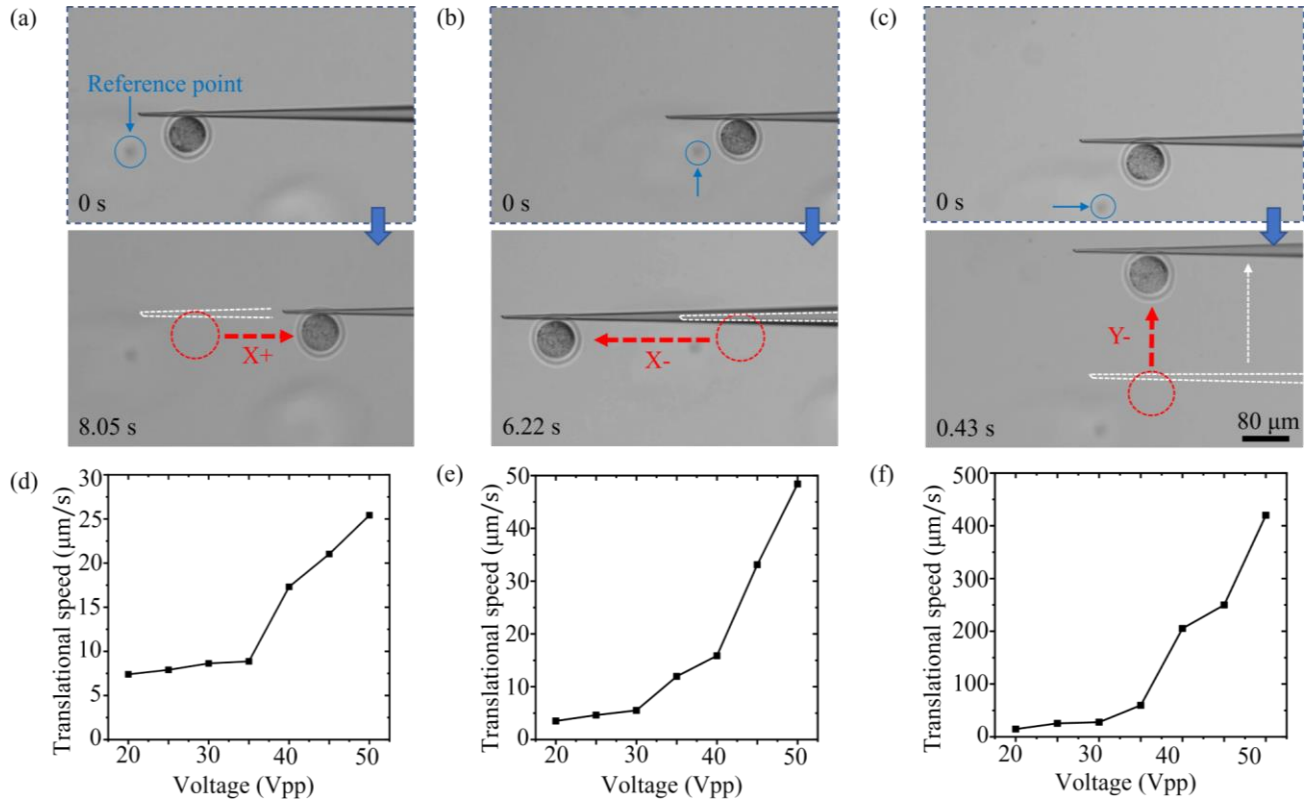

Figure 5. Transporting oocytes in different directions on the X-Y plane. (a)-(c) illustrate the translational process in X+, X- and Y- directions. The blue circles show the reference point. (d)-(e) are plots of the speed against input voltage in X+, X- and Y- directions.

and finally, it will be balanced at the below one under the influence of gravity.

The driven voltage applied to the PZT had an apparent effect on the rotation speed of the oocyte. We locked the input frequency at 3.6 kHz while changing the voltage from 0 to 60 V_{pp}, and measured the rotation speed at 10 V_{pp} intervals. The speed value was positively correlated with the voltage, as shown in Fig. 4(b). The minimum voltage that has enough force to drive rotation is 20 V_{pp}, and the revolutions per second (rps) rises quadratically with the input voltage increasing linearly, which can be confirmed by the red fitting line in the graph. In addition, the maximum applied voltage is 60 V_{pp} in the experiment. Higher voltages can result in higher rotational velocity, but excessive rotational force may damage cellular structures. Therefore, we restricted the voltage to ensure the biological activity of the oocytes.

With the quantitative relation of the input voltage and rotation speed, the angle of the oocyte posture can be accurately adjusted by controlling, and the input time of the signal at a proper voltage. Furthermore, by applying low voltage, the pipette can provide gentle contactless streaming to drive oocytes. We believe the controllability and flexibility of rotation make this method an advanced tool for the manipulation and research of oocytes and even other biological micro-objects.

B. Transportation in various directions

Before fine surgery of the single cell, transportation and positioning of targets are the most significant operations. For example, in oocyte intracellular injection, the target oocyte needs to be delivered to the work area where the micropipettes can reach to execute subsequent operations. A normal method is using the object stage to move the glass slide, and the oocyte will be transported with the glass slide. However, this method cannot change the relative position of the oocyte on the glass substrate. If the oocyte is at the edge of the medium droplet, it will be difficult to observe clearly and carry out surgery. The holding pipette, on the other hand, can hold and move the oocyte freely in various directions by using negative pressure. But it needs another 3-DOF manipulator to motor the holding pipette, which is not economical.

In the experiment, we were going to achieve transportation and positioning of a single oocyte only by utilizing the injection pipette and the acoustic waves, which means the holding pipette can be completely fixed without setting any motor. The oocyte was put in a medium droplet at the bottom with a reference point nearby, as shown in Fig. 5. The micropipette approached the oocyte and turned on the input signal, then indirectly captured the target with streaming and the radiation force. Importantly, the approaching process must be careful not to touch the oocyte surface, because the mutual contact in liquid may cause adhesive force between them, which makes the next step difficult to release the target. Once the microstreaming is activated, the flow will prevent both contact or moving away. When the target is moved to the destination, turning off the input acoustic signal can release it immediately to achieve the transportation task. Fig. 5(a)-(c) show processes of transporting oocytes on the X-Y plane, including translations that pointed in different directions. The input frequency chosen for the experiment is also 3.6 kHz to keep the target stable near the tip.

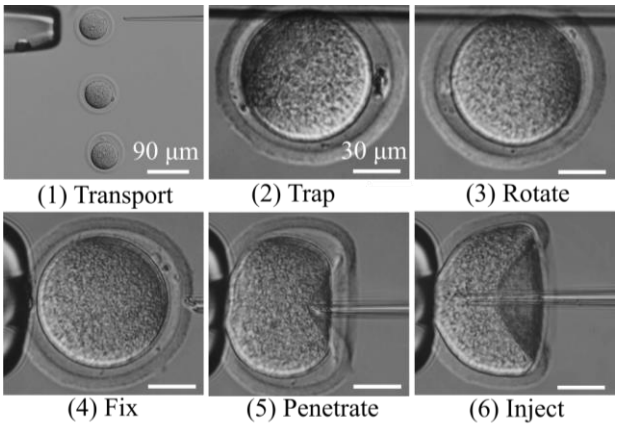

Figure 6. Process of hydrodynamic manipulations for injecting multiple oocytes.

To illustrate the transportation ability of the proposed acoustic manipulation method, the maximum delivery velocity of the oocyte was quantified as a main parameter to evaluate the efficiency and guide precise positioning. We only tested and recorded the maximum translational velocities of oocytes in X+, X- and Y- directions, as shown by arrows in Fig. 3. In Y-, the oocyte movements were as fast as the micropipette tip without leaving, even the manipulator motor was up to its maximum speed. It can be explained by the reason that the oocyte was pushed by a support force apart from the hydrodynamic force.

The graphs of Fig. 5(d)-(f) illustrate the relation of the input voltage and maximum translational speed in the three directions above, which can represent the transportation efficiency quantificationally. The value of the input voltage was set from 20 to 50 V_{pp}, and measured the maximum translational speed at 5 V_{pp} intervals. The translational speeds are positively correlated with the voltage, but their values show large differences when comparing the same voltage data from various directions. We speculate that the acoustic vortices would provide larger fluid force in the direction perpendicular to the rotation axis, but less force in the parallel direction. Although the efficiencies are not the same in various directions, the driven speed of oocytes can fulfill the requirements of flexibly positioning when using the injection pipette as a transportation tool only.

C. Process of Manipulation for Oocyte Injection

To confirm the availability and efficiency of the acoustical method for cell surgery, we utilized the proposed transportation and rotation process to manipulate multiple oocytes and facilitate the operations of injection. The detailed operating steps are shown in Fig. 6. The injection micropipette with an inner diameter of 10 μm is on the right, which has 3 DOF to capture and deliver oocytes in the acoustic field. The holding micropipette on the left was immobilized and connected to a microinjector, which only played roles in fixing targets and providing support force when injecting.

After putting several oocytes (N=12) in the medium droplet, the locations of them were observed by the microscope. We needed to transport the scattered oocytes to the position near the holding pipette. In the first step, the injection pipette tip was driven to deliver the oocyte by the acoustic force. The oocytes were moved to a place near the holding pipette tip as shown in Fig. 6, to increase the efficiency of the next operations. The intervals of each oocyte were set to more than 100 μm, in case of interference from the acoustic streaming

Secondly, the injection pipette tip approached an oocyte to the position sidelong with the acoustic waves off, then applied a low input voltage to rotate the oocyte slowly. When the poly body was adjusted to the focal plane and stayed away from the invasive site, the input acoustical signals were turned off immediately. In the next step, negative air pressure was slowly applied by a microinjector in the holding pipette to fix the oocyte. Finally, the operation of injecting can be executed easily due to the manipulations mentioned before. Repeating the above procedures until all the oocytes are transported and rotated to the appropriate position and posture, the overall time of finishing transportation and rotation were recorded respectively.

IV. Results and Discussion

There are three element functions of the acoustic method for hydrodynamic manipulation are evaluated in experiments, including contactless trapping, precise rotation, and two-dimensional transportation. With an input frequency of 3.6 kHz, if the driven voltage is larger than 20 V, the acoustically driven micropipette can trap the oocyte near the tip in a stable rotating status. Applying other values of frequencies can appear in various phenomena. During the process of testing frequencies, With some frequencies, the oocyte will be trapped at other locations along the pipette in some situations, but in most situations, the acoustic streaming will push close objects away. The possible reason is that most shapes of streaming cannot generate the proper vortices to trap oocytes.

By measuring the rotation speed of various applied voltages, the time of turning an oocyte per round can range from 4.6 s to less than 0.5 s, which means we can rotate the oocyte any degree of angle in a controllable time, as long as the applied voltage is proper. Compared to the typical operation of posture adjustment, using acoustic streaming to rotate is more efficient, controllable, and unharmful.

The 3.6 kHz frequency also was used to transport mouse oocytes. The translational speed rises nonlinearly with the driven voltage increasing, but the curves do not perfectly match the quadratic equation as the rotation speed does. One possible explanation is that the hydraulic resistance influences the movement of oocytes, which can be reflected by the noticeable slope increase at about 40 V_{pp}. Furthermore, the maximum velocities of translational movement along the X-axis are much less than those along the Y-axis, even when applied the same voltages. We speculate that the structures of the streaming are the main reason for these differences. The maximum delivery speed was tested to be 420 μm/s in Y-direction with the voltage of 50 V_{pp}. In general, a normal speed of less than 30 μm/s is enough for most single oocyte operations. We also tested the transportation in the Z axis and found that a voltage larger than 35 V_{pp} can make the micropipette lift an oocyte with acoustic radiation force.

Using the proposed hydrodynamic method, we transported 12 oocytes. After that, we fulfill the posture adjustments of all the oocytes one by one. In general, the oocyte manipulations of capture, movement, and posture adjustment can be fulfilled with a single acoustically driven pipette. The acoustic streaming not only can manipulate the target efficiently, but has universal applications in cell surgery, because of its low cost, easy operation, and high level of biocompatibility.

V. Conclusion

This paper proposes a noninvasive method to manipulate mouse oocytes with acoustic radiation force and streaming generated by the acoustic waves. The method employed an injection pipette to excite streaming in a droplet on the glass slide, equipped with a PZT to emit acoustic waves. The device can trap oocytes, precisely rotate, and transport them with an applied frequency of 3.6 kHz. The rotation speed and maximum transportation speed can be controlled by the input voltage.

Precise and controlled manipulation of cells is one of the important tasks in clinical and biology fields. Compared to the existing micromanipulation method for cell manipulation, our acoustic-driven manipulation method shows advances in delivery and posture adjustment of micro-targets, for it can operate oocytes with the advantages of high efficiency, controllability, non-invasion, and economy.

In future work, we will analyze the phenomenon caused by various frequencies, and figure out how to trap or release micro-targets by changing the input frequencies. Also, the oocyte movement in the vertical direction is inclined to be tested for executing the 3D transportation in the following studies. Furthermore, we tend to combine robotic methods such as visual servo control to manipulate biological targets automatically.

References

[1] C. Leung, Z. Lu, X. P. Zhang, and Y. Sun, "Three-Dimensional Rotation of Mouse Embryos," *IEEE Trans. Biomed. Eng.*, vol. 59, no. 4, pp. 1049–1056, Apr. 2012.

[2] A. G. Fraser, R. S. Kamath, P. Zipperlen, M. Martinez-Campos, M. Sohrmann, and J. Ahringer, "Functional genomic analysis of C. elegans chromosome I by systematic RNA interference," *Nature*, vol. 408, no. 6810, pp. 325–330, Nov. 2000.

[3] R. W. Carlsen and M. Sitti, "Bio-hybrid cell-based actuators for microsystems," *Small*, vol. 10, no. 19, pp. 3831–3851, 2014.

[4] S. Golfier, P. Rosendahl, A. Mietke, M. Herbig, J. Guck, and O. Otto, "High-throughput cell mechanical phenotyping for label-free titration assays of cytoskeletal modifications," *Cytoskeleton*, vol. 74, no. 8, pp. 283–296, 2017.

[5] T. Cacace, P. Memmolo, M. M. Villone, M. De Corato, M. Mugnano, M. Paturzo, P. Ferraro, and P. L. Maffettone, "Assembling and rotating erythrocyte aggregates by acoustofluidic pressure enabling full phase-contrast tomography," *Lab Chip*, vol. 19, no. 18, pp. 3123–3132, 2019.

[6] S. Miao, D. Chen, Q. Nie, X. Jiang, X. Sun, J. Dai, Y.-H. Liu, and X. Li, "Development of a vision-based robotic manipulation system for transferring of oocytes," in *2021 IEEE/RSJ international conference on intelligent robots and systems (IROS)*, 2021, pp. 7470–7475.

[7] X. Liu, Q. Shi, Y. Lin, M. Kojima, Y. Mae, T. Fukuda, Q. Huang, and T. Arai, "Multifunctional noncontact micromanipulation using whirling flow generated by vibrating a single piezo actuator," *Small*, vol. 15, no. 5, p. 1804421, 2019.

[8] Y. H. Anis, M. R. Holl, and D. R. Meldrum, "Automated selection and placement of single cells using vision-based feedback control," *IEEE Transactions on Automation Science and Engineering*, vol. 7, no. 3, pp. 598–606, 2010.

[9] P. Rubino, P. Viganò, A. Luddi, and P. Piomboni, "The ICSI procedure from past to future: a systematic review of the more controversial aspects," *Human Reproduction Update*, vol. 22, no. 2, pp. 194–227, Mar. 2016.

[10] C. Dai, G. Shan, H. Liu, C. Ru, and Y. Sun, "Robotic Manipulation of Sperm as a Deformable Linear Object," *IEEE Trans. Robot.*, vol. 38, no. 5, pp. 2799–2811, Oct. 2022.

[11] C. Dai, Z. Zhang, Y. Lu, G. Shan, X. Wang, Q. Zhao, C. Ru, and Y. Sun, "Robotic Manipulation of Deformable Cells for Orientation Control," *IEEE Trans. Robot.*, vol. 36, no. 1, pp. 271–283, Feb. 2020.

[12] X. Tang, X. Liu, P. Li, D. Liu, M. Kojima, Q. Huang, and T. Arai, "Efficient single-cell mechanical measurement by integrating a cell arraying microfluidic device with magnetic tweezer," *IEEE Robotics and Automation Letters*, vol. 6, no. 2, pp. 2978–2984, 2021.

[13] X. Wang, C. Ho, Y. Tsatskis, J. Law, Z. Zhang, M. Zhu, C. Dai, F. Wang, M. Tan, S. Hopyan, H. McNeill, and Y. Sun, "Intracellular manipulation and measurement with multipole magnetic tweezers," *Science Robotics*, vol. 4, no. 28, p. eaav6180, Mar. 2019.

[14] L. Gu, S. K. Mohanty, and N. Ingle, "Detachment and reorientation of cells using near-infrared laser microbeam," *Journal of Biomedical Optics*, vol. 16, no. 11, p. 115002, 2011.

[15] S. Mohanty, "Optically-actuated translational and rotational motion at the microscale for microfluidic manipulation and characterization," *Lab Chip*, vol. 12, no. 19, pp. 3624–3636, 2012.

[16] A. Thakur, S. Chowdhury, P. Švec, C. Wang, W. Losert, and S. K. Gupta, "Indirect pushing based automated micromanipulation of biological cells using optical tweezers," *The International Journal of Robotics Research*, vol. 33, no. 8, pp. 1098–1111, 2014.

[17] Z. Chen, X. Liu, X. Tang, Y. Li, D. Liu, Y. Li, Q. Huang, and T. Arai, "On-chip automatic trapping and rotating for zebrafish embryo injection," *IEEE Robotics and Automation Letters*, vol. 7, no. 4, pp. 10850–10856, 2022.

[18] Z. Wang, C. Feng, R. Muruganandam, J. Mathew, P. C. Wong, W. T. Ang, S. Y. M. Tan, and W. T. Latt, "A fully automated robotic system for three-dimensional cell rotation," in *2016 IEEE International Conference on Robotics and Automation (ICRA)*, Stockholm, Sweden, 2016, pp. 1707–1712.

[19] Z. Wang, C. Feng, R. Muruganandam, W. T. Ang, S. Y. M. Tan, and W. T. Latt, "Three-Dimensional Cell Rotation With Fluidic Flow-Controlled Cell Manipulating Device," *IEEE/ASME Trans. Mechatron.*, vol. 21, no. 4, pp. 1995–2003, Aug. 2016.

[20] P. Zhang, C. Chen, F. Guo, J. Philippe, Y. Gu, Z. Tian, H. Bachman, L. Ren, S. Yang, Z. Zhong, P.-H. Huang, N. Katsanis, K. Chakrabarty, and T. J. Huang, "Contactless, programmable acoustofluidic manipulation of objects on water," *Lab Chip*, vol. 19, no. 20, pp. 3397–3404, 2019.

[21] S. P. Zhang, J. Lata, C. Chen, J. Mai, F. Guo, Z. Tian, L. Ren, Z. Mao, P.-H. Huang, P. Li, S. Yang, and T. J. Huang, "Digital acoustofluidics enables contactless and programmable liquid handling," *Nature Communications*, vol. 9, no. 1, p. 2928, Jul. 2018.

[22] P. Li and T. J. Huang, "Applications of Acoustofluidics in Bioanalytical Chemistry," *Anal. Chem.*, vol. 91, no. 1, pp. 757–767, Jan. 2019.

[23] J. Durrer, P. Agrawal, A. Ozgul, S. C. F. Neuhauss, N. Nama, and D. Ahmed, "A robot-assisted acoustofluidic end effector," Nature Communications, vol. 13, no. 1, p. 6370, Oct. 2022.

[24] S. Li, Y. Wei, F. Qu, G. Zhang, W. Pang, and W. Cui, "Vibration mode tuning of acoustic pillar array chip for precise microscale manipulations," in *2022 IEEE international ultrasonics symposium (IUS)*, 2022, pp. 1–4.

[25] H. Bruus, "Acoustofluidics 7: The acoustic radiation force on small particles," *Lab Chip*, vol. 12, no. 6, pp. 1014–1021, 2012.